Preprint – IJCAI 2025: This is the accepted version made available for conference attendees.
Do not cite. The final version will appear in the IJCAI 2025 proceedings.

Flexible Generalized Low-Rank Regularizer for Tensor RPCA

Zhiyang Gong[1*], **Jie Yu**[1*], **Yutao Hu**[1], **Yulong Wang**[1,2,3†]
[1] College of Informatics, Huazhong Agricultural University, China
[2] Engineering Research Center of Intelligent Technology for Agriculture, Ministry of Education, China
[3] Key Laboratory of Smart Farming Technology for Agricultural Animals, Ministry of Agriculture and Rural Affairs, China
{zhiyanggong499, jieyu.gm, yutaohu0216, wangyulong6251}@gmail.com

Abstract

Tensor Robust Principal Component Analysis (TRPCA) has emerged as a powerful technique for low-rank tensor recovery. To achieve better recovery performance, a variety of TNN (Tensor Nuclear Norm) based low-rank regularizers have been proposed case by case, lacking a general and flexible framework. In this paper, we design a novel tensor low-rank regularization framework coined FGTNN (Flexible Generalized Tensor Nuclear Norm). Equipped with FGTNN, we develop the FGTRPCA (Flexible Generalized TRPCA) framework, which has two desirable properties. 1) Generalizability: Many existing TRPCA methods can be viewed as special cases of our framework; 2) Flexibility: Using FGTRPCA as a general platform, we derive a series of new TRPCA methods by tuning a continuous parameter to improve performance. In addition, we develop another novel smooth and low-rank regularizer coined t-FGJP and the resulting SFGTRPCA (Smooth FGTRPCA) method by leveraging the low-rankness and smoothness priors simultaneously. Experimental results on various tensor denoising and recovery tasks demonstrate the superiority of our methods.

1 Introduction

Tensor data are ubiquitous, many real-world data are usually inherently multidimensional, with information stored in multi-way arrays known as tensors, e.g., images, videos, network flow data, etc. In recent years, significant advancements across various interdisciplinary domains have been made in tensor analysis, such as machine learning [Wen *et al.*, 2024; Phothilimthana *et al.*, 2024], data mining [Zhang *et al.*, 2023a; Huang *et al.*, 2024], and computer vision [Zhao *et al.*, 2024; Liu *et al.*, 2024a]. However, due to the inherent limitations of signal acquisition equipment, including sensor sensitivity, photon effects, and calibration errors, tensor data gathered from real-world environments frequently suffer from substantial corruption [Wang *et al.*, 2023a]. Consequently, tensor recovery has become a crucial task in tensor analysis.

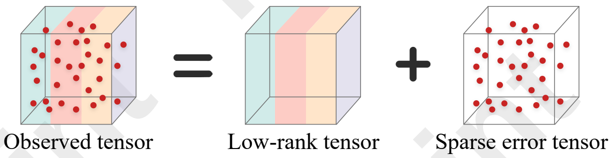

Figure 1: An illustration of TRPCA, which demonstrates the decomposition of observation tensor into low-rank and sparse components.

This paper concentrates on the problem of Tensor Robust Principal Component Analysis (TRPCA) [Huang *et al.*, 2015], which seeks to recover the underlying low-rank tensor $\boldsymbol{\mathcal{L}}$ and sparse tensor $\boldsymbol{\mathcal{E}}$ from their sum $\boldsymbol{\mathcal{M}}$ (see Figure 1 for a visual representation) and solves the following problem

$$\min_{\boldsymbol{\mathcal{L}},\boldsymbol{\mathcal{E}}\in\mathbb{R}^{d_1\times d_2\times d_3}} \text{rank}(\boldsymbol{\mathcal{L}}) + \lambda\|\boldsymbol{\mathcal{E}}\|_1 \ \text{ s.t. } \boldsymbol{\mathcal{M}} = \boldsymbol{\mathcal{L}} + \boldsymbol{\mathcal{E}}, \quad (1)$$

where $\lambda > 0$ is a regularization parameter, rank($\boldsymbol{\mathcal{L}}$) denotes the rank of clean tensor $\boldsymbol{\mathcal{L}}$ and $\|\boldsymbol{\mathcal{E}}\|_1$ is ℓ_1-norm (sum of the absolute values of all the entries) to measure the sparsity of the noise tensor $\boldsymbol{\mathcal{E}}$. A key challenge is the definition of tensor rank, which is inherently more complex than matrix rank. Various conventional methods for defining tensor rank originate from distinct tensor decompositions. For instance, inspired by the tensor singular value decomposition (t-SVD), [Kilmer *et al.*, 2013] proposed the tensor tubal rank that can be efficiently computed using the fast Fourier Transform (FFT). Since the non-convexity and discontinuity of the rank function, solving the problem (1) is usually NP-hard. Consequently, [Lu *et al.*, 2020] proposed a novel tensor nuclear norm as a convex approximation to the tensor tubal rank and proposed a new TRPCA method defined as follows

$$\min_{\boldsymbol{\mathcal{L}},\boldsymbol{\mathcal{E}}} \|\boldsymbol{\mathcal{L}}\|_* + \lambda\|\boldsymbol{\mathcal{E}}\|_1 \ \text{ s.t. } \boldsymbol{\mathcal{M}} = \boldsymbol{\mathcal{L}} + \boldsymbol{\mathcal{E}}, \quad (2)$$

where $\|\cdot\|_*$ represents the tensor nuclear norm (TNN). Furthermore, recent research by [Kilmer *et al.*, 2021] has demonstrated the optimal representation and compression capabilities of t-SVD, further highlighting the significance of model (2) in capturing the intrinsic low-rank structures of tensors. As a result, the model (2) under t-SVD has garnered considerable interests recently [Hou *et al.*, 2024; Liu *et al.*, 2024c; Qin *et al.*, 2024].

†Corresponding author: Yulong Wang

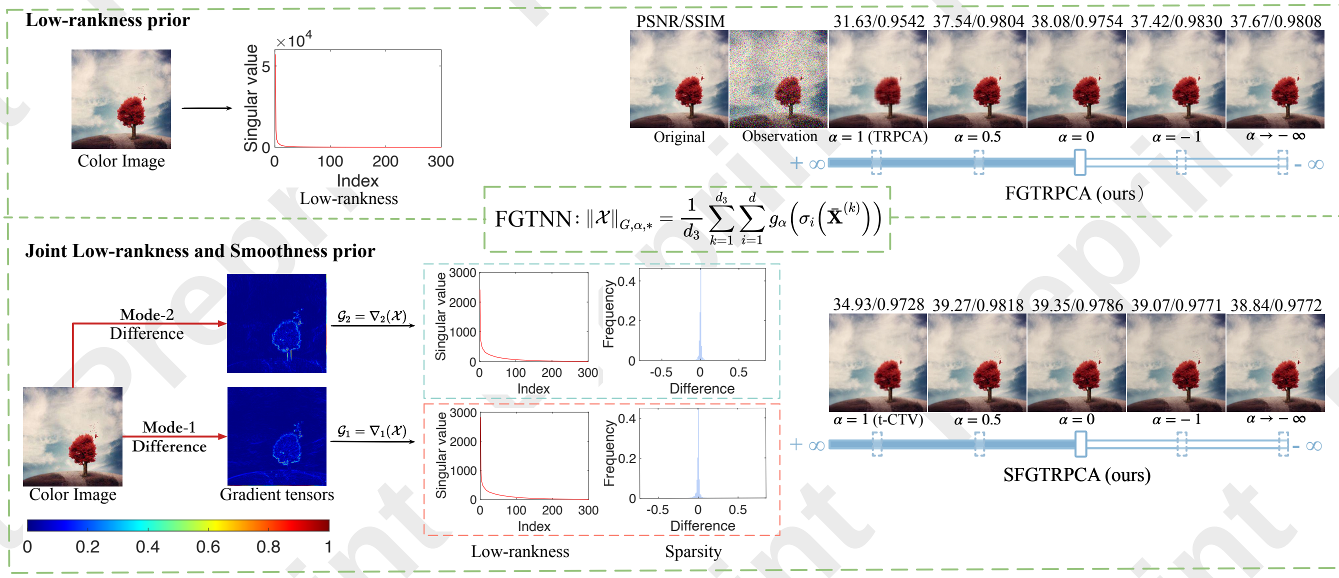

Figure 2: Take a color image sample from ZJU dataset as an example. The two frames illustrate the recovery performance of our proposed FGTRPCA and SFGTRPCA with different values of shape parameter α (see Eq. (5)) under different structure priors of color images.

Despite the impressive performance of TRPCA, it still exhibits several limitations. Specifically, when minimizing the TNN, TRPCA employs tensor singular value thresholding to uniformly diminish all singular values. In real-world applications, singular values often carry distinct physical meanings, supported by prior knowledge indicating that larger singular values are generally associated with more significant information. The uniform shrinkage approach of TRPCA fails to account for these differences among singular values, potentially leading to suboptimal results.

While many existing advanced methodologies [Gao *et al.*, 2020; Jiang *et al.*, 2020; Wang *et al.*, 2023b; Zhang *et al.*, 2023b; Yan and Guo, 2024; Liu *et al.*, 2024b] develop various TNN-based low-rank regularizers that penalize large singular values less and small singular values more, thereby efficiently preserving essential information and filtering out irrelevant details. However, their discrete and fixed models lack flexibility for diverse scenarios. To address this problem, we design a novel Flexible Generalized low-rank regularizer (FGTNN) to adaptively assign different penalties to distinct singular values and impose the constraint on the sparse component. We have shown that several existing TRPCA models can be reformulated as special cases of FGTRPCA. Apart from that, we can also derive a wider family of new TRPCA models by tuning a continuous parameter to improve performance. Through this, our model significantly improves flexibility and efficiency in complex situations.

Note that the low-rankness prior and the smoothness prior modeled by total variation (TV) are widely utilized in tensor recovery applications [Ko *et al.*, 2020; Qiu *et al.*, 2021]. This prior states how similar objects/scenes (with shapes) are adjacently distributed [Peng *et al.*, 2022b]. Most previous works encoded the two priors with two independent regularizers and incorporated them into a unified model, which achieved better performance [Peng *et al.*, 2020; Peng *et al.*, 2022a]. However, they have two drawbacks: (1) it is challenging to fine-tune the regularization parameter between the two terms; (2) the theoretical guarantee for exact recovery remains unproven for the related methods.

Given the circumstances above, [Wang *et al.*, 2023a] proposed the tensor Correlated Total Variation (t-CTV) norm which integrates the two priors into a single regularization term, eliminating the need for tuning separate parameters. Moreover, this work offered theoretical guarantees for the precise recovery of analogous tensor methods that concurrently model both priors. Analogously, the integration regularization term was also based on TNN in the gradient domain. Consequently, [Huang *et al.*, 2024] proposed a reweighted regularizer based on ℓ_p norm as a surrogate for t-CTV term. In this paper, we employ FGTNN to explore the inherent structural properties of gradient tensors and introduce a new tensor-correlated Flexible Generalized Joint Prior (t-FGJP) regularizer.

Our principal contributions are outlined as follows:

- We propose a flexible generalized low-rank regularizer (FGTNN) that accounts for the varying importance of different singular values in low-rank tensors and develop a novel FGTRPCA framework. The FGTRPCA, not only regards many existing TRPCA methods as special cases, but also opens a door to design a broad new family of TRPCA methods by tuning a continuous parameter. This enhances the flexibility of our model to counter more intricate scenarios.
- Considering the low-rankness and smoothness priors simultaneously, we propose a novel tensor-correlated Flexible Generalized Joint Prior (t-FGJP) regularizer based on FGTNN. It maintains the flexibility of discriminatively controlling different singular values of the gradient tensors and can derive a new smooth FGTRPCA

model, termed SFGTRPCA.

- We design ADMM-based [Boyd *et al.*, 2011] optimization algorithmic frameworks tailored for our FGTRPCA and SFGTRPCA models. Extensive experiments on various tensor denoising and recovery tasks demonstrate the advantages of our models.

2 Notations and Preliminaries

First, we present some key notations and definitions used throughout the paper. We represent scalars, vectors, and matrices using lowercase letters, boldface lowercase letters, and boldface uppercase letters, e.g., x, $\mathbf{x}$, $\mathbf{X}$, respectively. Tensors are presented by bold calligraphic letters, e.g., $\boldsymbol{\mathcal{X}}$. $\mathbf{1}_{d_1\times d_2}$ and $\mathbf{1}_{d_1\times d_2\times d_3}$ represent a matrix of size $d_1\times d_2$ and a tensor of size $d_1\times d_2\times d_3$ with all entries as ones. For a 3-order tensor $\boldsymbol{\mathcal{X}}\in\mathbb{R}^{d_1\times d_2\times d_3}$, we denote $\boldsymbol{\mathcal{X}}_{ijk}$ as its (i,j,k)-th entry, $\boldsymbol{\mathcal{X}}(i,:,:)$ as its horizontal slice, $\boldsymbol{\mathcal{X}}(:,j,:)$ as its lateral slice, $\boldsymbol{\mathcal{X}}(:,:,k)$ as its frontal slice, respectively. For convenience, the frontal slice $\boldsymbol{\mathcal{X}}(:,:,k)$ is often denoted as $\mathbf{X}^{(k)}$. The tensor nuclear norm (TNN), tensor ℓ_1 norm (TL1N), tensor Frobenius norm and tensor infinity norm of $\boldsymbol{\mathcal{X}}$ are defined by $\|\boldsymbol{\mathcal{X}}\|_*$, $\|\boldsymbol{\mathcal{X}}\|_1=\sum_{ijk}|\boldsymbol{\mathcal{X}}_{ijk}|$, $\|\boldsymbol{\mathcal{X}}\|_F=\sqrt{\sum_{ijk}|\boldsymbol{\mathcal{X}}_{ijk}|^2}$ and $\|\boldsymbol{\mathcal{X}}\|_\infty=\max_{ijk}|\boldsymbol{\mathcal{X}}_{ijk}|$, respectively. The transpose of $\boldsymbol{\mathcal{X}}$ is defined as $\boldsymbol{\mathcal{X}}^T\in\mathbb{R}^{d_2\times d_1\times d_3}$ [Lu *et al.*, 2020].

Definition 1. ***(T-SVD)*** *[Kilmer and Martin, 2011] For a tensor $\boldsymbol{\mathcal{X}}\in\mathbb{R}^{d_1\times d_2\times d_3}$, it can be factorized by t-SVD as*

$$\boldsymbol{\mathcal{X}}=\boldsymbol{\mathcal{U}}*\boldsymbol{\mathcal{S}}*\boldsymbol{\mathcal{V}}^T, \tag{3}$$

where $\boldsymbol{\mathcal{U}}\in\mathbb{R}^{d_1\times d_1\times d_3}$, $\boldsymbol{\mathcal{V}}\in\mathbb{R}^{d_2\times d_2\times d_3}$ are orthogonal tensors, i.e., $\boldsymbol{\mathcal{U}}*\boldsymbol{\mathcal{U}}^T=\boldsymbol{\mathcal{U}}^T*\boldsymbol{\mathcal{U}}=\boldsymbol{\mathcal{V}}*\boldsymbol{\mathcal{V}}^T=\boldsymbol{\mathcal{V}}^T*\boldsymbol{\mathcal{V}}=\boldsymbol{\mathcal{I}}$, and $\boldsymbol{\mathcal{S}}\in\mathbb{R}^{d_1\times d_2\times d_3}$ is an f-diagonal tensor, i.e., each frontal slices are the diagonal matrices, and "$*$" is the t-product.

Definition 2. ***(Tensor Nuclear Norm, TNN)*** *[Lu* et al.*, 2020] For a tensor $\boldsymbol{\mathcal{X}}\in\mathbb{R}^{d_1\times d_2\times d_3}$, $d=\min(d_1,d_2)$, the Tensor Nuclear Norm of $\boldsymbol{\mathcal{X}}$ is defined as*

$$\|\boldsymbol{\mathcal{X}}\|_*=\frac{1}{d_3}\sum_{k=1}^{d_3}\sum_{i=1}^{d}\sigma_i\left(\bar{\mathbf{X}}^{(k)}\right), \tag{4}$$

where $\bar{\boldsymbol{\mathcal{X}}}$ is the result by applying FFT on $\boldsymbol{\mathcal{X}}$ along the third dimension, i.e., $\bar{\boldsymbol{\mathcal{X}}}=fft(\boldsymbol{\mathcal{X}},[],3)$. $\bar{\mathbf{X}}^{(k)}$ is the k-th frontal slice of $\bar{\boldsymbol{\mathcal{X}}}$, $\sigma_i\left(\bar{\mathbf{X}}^{(k)}\right)$ is the i-th singular value of $\bar{\mathbf{X}}^{(k)}$.

3 Proposed Methods

We begin by detailing the motivation for FGTNN and its characteristics, then propose the FGTRPCA framework and implement it using an efficient optimization algorithm. Furthermore, by simultaneously considering low-rankness and smoothness priors, we develop a novel t-FGJP regularizer and apply it to solve TRPCA problem, termed SFGTRPCA.

3.1 Flexible Generalized TNN

According to Definition 2, the original TNN uniformly shrinks each singular value of the low-rank tensor $\boldsymbol{\mathcal{L}}$ when minimizing the tensor nuclear norm, which may lead to suboptimal solution. Indeed, larger singular values are associated with more critical information within the tensor. Inspired by the common purposes of enhancing TRPCA methods, we introduce a flexible generalized tensor nuclear norm (FGTNN) as a unified framework, which is defined below.

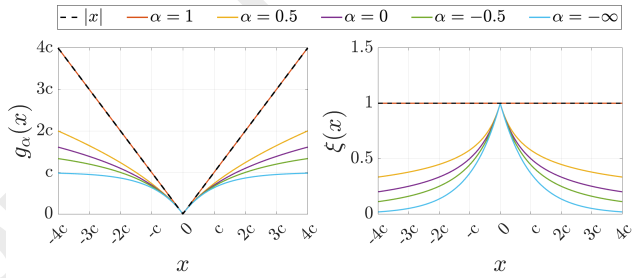

Figure 3: $g_\alpha(x)$ and its corresponding weight function $\xi(x)$.

Definition 3. ***(FGTNN)*** *For a tensor $\boldsymbol{\mathcal{X}}\in\mathbb{R}^{d_1\times d_2\times d_3}$, $d=\min(d_1,d_2)$, the Flexible Generalized Tensor Nuclear Norm (FGTNN) is defined as follows*

$$\|\boldsymbol{\mathcal{X}}\|_{G,\alpha,*}=\frac{1}{d_3}\sum_{k=1}^{d_3}\sum_{i=1}^{d}g_\alpha\left(\sigma_i\left(\bar{\mathbf{X}}^{(k)}\right)\right), \tag{5}$$

where $g_\alpha(x)$ follows [Barron et al.*, 2023]:*

$$g_\alpha(x)=c\cdot\frac{|\alpha-1|}{\alpha}\left(\left(\frac{|x|/c}{|\alpha-1|}+1\right)^\alpha-1\right), \tag{6}$$

where $\alpha\in\mathbb{R}$ is a continuous parameter that controls the shape of $g_\alpha(x)$ and $c>0$ is a scale parameter.

Remark 1. *Our proposed FGTNN mainly exhibits two desirable properties.* ***1) Generalizability****: By introducing a continuous parameter α, low-rank regularizers in many existing popular methods such as TRPCA, LRTF, ETR, and DATRPCA can be viewed as special cases of FGTNN with different values of α.(see Table 1 for more details);* ***2) Flexibility****: We can develop plenty of new low-rank regularizers by tuning α and achieve better performance. Compared to the method with fixed-form low-rank regularizer, our model gains flexibility and can adapt to more complex scenarios. Apart from that, $g_\alpha(x)$ in FGTNN controls the penalty strength to singular values. Figure 3(a) intuitively presents the characteristics of $g_\alpha(x)$. We observe that $g_\alpha(x)$ increases slower than $|x|$ for various α, which means less shrunk to large singular values, preserving the critical information within the tensor to a greater extent. More importantly, α is related to the shape of $g_\alpha(x)$. When $\alpha\to-\infty$, $g_\alpha(x)$ follows an approximately exponential form; When $\alpha=0$, $g_\alpha(x)$ takes a logarithmic form; When $\alpha=1$, $g_\alpha(x)$ turns to $|x|$; And in the other case of α, $g_\alpha(x)$ is represented in a approximate power form.*

Specifically, we can extend FGTNN to the sparse component and define the flexible generalized tensor ℓ_1 norm (FGTL1N).

Definition 4. ***(FGTL1N)*** *For a tensor $\boldsymbol{\mathcal{X}}\in\mathbb{R}^{d_1\times d_2\times d_3}$, the Flexible Generalized Tensor ℓ_1 Norm (FGTL1N) is defined as follows:*

$$\|\boldsymbol{\mathcal{X}}\|_{G,\alpha,1}=\sum_{i=1}^{d_1}\sum_{j=1}^{d_2}\sum_{k=1}^{d_3}g_\alpha\left(|\boldsymbol{\mathcal{X}}_{ijk}|\right). \tag{7}$$

Author and year	Method	Value of α	$g_\alpha(x)$	Low-rank Regularizer
[Lu *et al.*, 2020]	TRPCA	$\alpha = 1$	$\|x\|$	$\|\boldsymbol{\mathcal{X}}\|_{G,1,*}$
[Chen *et al.*, 2021]	LRTF	$\alpha = 0$	$c\ln(\|x\|/c+1)$	$\|\boldsymbol{\mathcal{X}}\|_{G,0,*}$
[Ji and Feng, 2023]	ETR	$\alpha = -1$	$\frac{2\|x\|}{\|x\|/c+2}$	$\|\boldsymbol{\mathcal{X}}\|_{G,-1,*}$
[Wang *et al.*, 2023b]	DATRPCA	$\alpha \to -\infty$	$c(1-\exp(-\|x\|/c))$	$\|\boldsymbol{\mathcal{X}}\|_{G,-\infty,*}$

Table 1: The FGTNN regularizer view for many special cases.

3.2 Flexible Generalized TRPCA

By integrating FGTNN and FGTL1N into the TRPCA framework, we formulate the following Flexible Generalized TRPCA (FGTRPCA) model.

$$\min_{\boldsymbol{\mathcal{L}},\boldsymbol{\mathcal{E}}\in\mathbb{R}^{d_1\times d_2\times d_3}} \|\boldsymbol{\mathcal{L}}\|_{G,\alpha,*}+\lambda\|\boldsymbol{\mathcal{E}}\|_{G,\alpha,1} \text{ s.t. } \boldsymbol{\mathcal{M}}=\boldsymbol{\mathcal{L}}+\boldsymbol{\mathcal{E}}. \quad (8)$$

Remark 2. *It is worth pointing out that FGTRPCA serves as a versatile framework for addressing TRPCA problems. By adjusting the parameter α, it can be tailored to develop new TRPCA methods. Specifically, in this paper, we introduce a variant of FGTRPCA with $\alpha = 0.5$, a choice that has not been explored before.*

Note that FGTNN includes a series of specific functions that are nonlinear and complex, thus making it hard to obtain the optimal solution of the FGTRPCA model. In this paper, we design an efficient algorithm optimization framework based on the ADMM framework [Boyd *et al.*, 2011] to implement the FGTRPCA model.

Proposition 1. *For $g_\alpha(x)$, there exists a convex conjugate function $\phi : \mathbb{R} \to \mathbb{R}$ which satisfies*

$$g_\alpha(x) = \min_{w\in\mathbb{R}_+} (w|x| + \phi(w)), \quad (9)$$

and for fixed x, the minimum is reached at $w = \xi(x;c)$(c is a positive constant), which is defined as

$$w=\xi(x;c)=\begin{cases}1, & \text{if } \alpha=1\\ c/(|x|+c), & \text{if } \alpha=0\\ \exp(-|x|/c), & \text{if } \alpha=-\infty\\ \left(\frac{|x|/c}{|\alpha-1|}+1\right)^{\alpha-1}, & \text{otherwise,}\end{cases} \quad (10)$$

Remark 3. *According to Proposition 1, $g_\alpha(x)$ in Eq. (6) can be optimized by an adaptive alternating weighted minimization scheme. From the perspective of weights, smaller weights represent smaller shrinkages to singular values. As shown in Figure 3(b), TNN assigns equal weight to each singular value, i.e., TNN treats each singular value equally. For our proposed FGTNN, larger singular values will adaptively receive smaller weights, resulting in less shrinkage.*

According to Proposition 1, FGTNN can be transformed into

$$\|\boldsymbol{\mathcal{L}}\|_{G,\alpha,*} = \min_{\mathbf{W}} \frac{1}{d_3}\sum_{k=1}^{d_3}\sum_{i=1}^{d}(W_{ki}\sigma_i(\bar{\mathbf{L}}^{(k)})+\phi(W_{ki})), \quad (11)$$

where the W_{ki} is the k,i-th element of matrix $\mathbf{W}\in\mathbb{R}^{d_3\times d}$. The minimum is reached at $W_{ki}=\xi(\sigma_i(\bar{\mathbf{L}}^{(k)});c)$. Similarly, as for FGTL1N, we have

$$\|\boldsymbol{\mathcal{E}}\|_{G,\alpha,1} = \min_{\boldsymbol{\mathcal{W}}}\sum_{i=1}^{d_1}\sum_{j=1}^{d_2}\sum_{k=1}^{d_3}(\boldsymbol{\mathcal{W}}_{ijk}|\boldsymbol{\mathcal{E}}_{ijk}|+\phi(\boldsymbol{\mathcal{W}}_{ijk})), \quad (12)$$

where the $\boldsymbol{\mathcal{W}}_{ijk}$ is the i,j,k-th element of tensor $\boldsymbol{\mathcal{W}}\in\mathbb{R}^{d_1\times d_2\times d_3}$. The minimum is reached at $\boldsymbol{\mathcal{W}}_{ijk}=\xi(|\boldsymbol{\mathcal{E}}_{ijk}|;c)$.

Notably, problem (8) can be reformulated as the weighted tensor nuclear norm minimization problem (11) and the weighted tensor ℓ_1 norm minimization problem (12). The following defines two key concepts: Weighted tensor nuclear norm (WTNN) and weighted tensor ℓ_1 norm (WTL1N).

Definition 5. ***(Weighted Tensor Nuclear Norm, WTNN)****[Wang* et al.*, 2023b] For a tensor $\boldsymbol{\mathcal{X}}\in\mathbb{R}^{d_1\times d_2\times d_3}$ and a weight matrix $\mathbf{W}\in\mathbb{R}^{d_3\times d}$, $d=\min(d_1,d_2)$, the WTNN of $\boldsymbol{\mathcal{X}}$ is defined as*

$$\|\boldsymbol{\mathcal{X}}\|_{\mathbf{W},*} = \frac{1}{d_3}\sum_{k=1}^{d_3}\sum_{i=1}^{d} W_{ki}\sigma_i\left(\bar{\mathbf{X}}^{(k)}\right). \quad (13)$$

Definition 6. ***(Weighted Tensor ℓ_1 Norm, WTL1N)****[Wang* et al.*, 2023b] For a tensor $\boldsymbol{\mathcal{X}}\in\mathbb{R}^{d_1\times d_2\times d_3}$ and a weight tensor $\boldsymbol{\mathcal{W}}\in\mathbb{R}^{d_1\times d_2\times d_3}$, the WTL1N of $\boldsymbol{\mathcal{X}}$ is defined as*

$$\|\boldsymbol{\mathcal{X}}\|_{\boldsymbol{\mathcal{W}},1} = \sum_{i=1}^{d_1}\sum_{j=1}^{d_2}\sum_{k=1}^{d_3}|\boldsymbol{\mathcal{W}}_{ijk}\boldsymbol{\mathcal{X}}_{ijk}|. \quad (14)$$

By incorporating Eq. (11) and Eq. (12) into model (8), and according to the definition of WTNN and WTL1N, we have

$$\min_{\boldsymbol{\mathcal{L}},\boldsymbol{\mathcal{E}},\mathbf{W},\boldsymbol{\mathcal{W}}} \|\boldsymbol{\mathcal{L}}\|_{\mathbf{W},*}+\lambda\|\boldsymbol{\mathcal{E}}\|_{\boldsymbol{\mathcal{W}},1}+\Phi_M(\mathbf{W})+\Phi_T(\boldsymbol{\mathcal{W}}) \\ \text{s.t. } \boldsymbol{\mathcal{M}}=\boldsymbol{\mathcal{L}}+\boldsymbol{\mathcal{E}}, \quad (15)$$

where $\Phi_M(\mathbf{W})$ and $\Phi_T(\boldsymbol{\mathcal{W}})$ are defined such that $\Phi_M(\mathbf{W}) = \sum_{k=1}^{d_1}\sum_{i=1}^{d_2}\psi(W_{ki})$ and $\Phi_T(\boldsymbol{\mathcal{W}}) = \sum_{i=1}^{d_1}\sum_{j=1}^{d_2}\sum_{k=1}^{d_3}\psi(\boldsymbol{\mathcal{W}}_{ijk})$. In the next part, we will present the optimization for implementing FGTRPCA.

3.3 Optimization for FGTRPCA

The Lagrangian function of the FGTRPCA model is

$$L(\boldsymbol{\mathcal{L}},\boldsymbol{\mathcal{E}},\mathbf{W},\boldsymbol{\mathcal{W}},\boldsymbol{\mathcal{Z}},\mu)=\|\boldsymbol{\mathcal{L}}\|_{\mathbf{W},*}+\lambda\|\boldsymbol{\mathcal{E}}\|_{\boldsymbol{\mathcal{W}},1}+\Phi_M(\mathbf{W}) \\ +\Phi_T(\boldsymbol{\mathcal{W}})+\frac{\mu}{2}\left\|\boldsymbol{\mathcal{L}}+\boldsymbol{\mathcal{E}}-\boldsymbol{\mathcal{M}}+\frac{\boldsymbol{\mathcal{Z}}}{\mu}\right\|_F^2-\frac{\mu}{2}\|\boldsymbol{\mathcal{Z}}/\mu\|_F^2, \quad (16)$$

where $\boldsymbol{\mathcal{Z}} \in \mathbb{R}^{d_1\times d_2\times d_3}$ denotes the Lagrangian multiplier and μ is a positive parameter. Each variable can be updated alternately in the scheme of the ADMM framework.

Step1: Update $\boldsymbol{\mathcal{L}}$ by fixing the other variables:

$$\boldsymbol{\mathcal{L}}_{t+1} = \arg\min_{\boldsymbol{\mathcal{L}}} \frac{1}{\mu_t}\|\boldsymbol{\mathcal{L}}\|_{\mathbf{W},*}+\frac{1}{2}\|\boldsymbol{\mathcal{L}}-(\boldsymbol{\mathcal{M}}-\boldsymbol{\mathcal{E}}_t-\boldsymbol{\mathcal{Z}}_t/\mu_t)\|_F^2. \tag{17}$$

The closed-form solution of (17) can be easily obtained with the following proximity operator.

Lemma 1. *Given $\boldsymbol{\mathcal{X}} \in \mathbb{R}^{d_1\times d_2\times d_3}$ with t-SVD $\boldsymbol{\mathcal{X}} = \boldsymbol{\mathcal{U}} * \boldsymbol{\mathcal{S}} * \boldsymbol{\mathcal{V}}^*$ and a weight matrix $\mathbf{W} \in \mathbb{R}^{d\times d_3}$, where $\mathbf{w}_k$ is the k-th column of $\mathbf{W}$ and $d = min\{d_1, d_2\}$. Considering the following Weighted Tensor Nuclear Norm minimization (WTNNM) problem*

$$\mathbf{Prox}_{\|\cdot\|_{\mathbf{W},*}}(\boldsymbol{\mathcal{X}}) = \arg\min_{\boldsymbol{\mathcal{L}}} \frac{1}{2}\|\boldsymbol{\mathcal{L}}-\boldsymbol{\mathcal{X}}\|_F^2 + \|\boldsymbol{\mathcal{L}}\|_{\mathbf{W},*}, \tag{18}$$

where $\|\cdot\|_{\mathbf{W},*}$ denotes the WTNN, and $\mathbf{Prox}_{\|\cdot\|_{\mathbf{W},*}}$ is defined as a proximal operator. For non-descending weights $0 \le W_{k1} \le W_{k2} \le \cdots \le W_{kd} (k = 1, \dots, d_3)$, the problem (18) *has the global solution which is defined as*

$$\boldsymbol{\mathcal{L}}^* = \mathbf{Prox}_{\|\cdot\|_{\mathbf{W},*}}(\boldsymbol{\mathcal{X}}) = \boldsymbol{\mathcal{U}} * ifft(\mathcal{P}_{\mathbf{W}}(\bar{\boldsymbol{\mathcal{S}}}), [], 3) * \boldsymbol{\mathcal{V}}^*, \tag{19}$$

where ifft denotes the inverse fast Fourier transform applied along the third dimension, $\mathcal{P}_{\mathbf{W}}(\bar{\boldsymbol{\mathcal{S}}})$ is a tensor to meet the conditions of its k-th frontal slice is $\mathbf{P}_{\mathbf{w}_k}(\bar{\mathbf{S}}^{(k)})$ for $k = 1, \dots, d_3$. $\bar{\mathbf{S}}^{(k)}$ is the k-th frontal slice of $\bar{\boldsymbol{\mathcal{S}}}$, and $\mathbf{P}_{\mathbf{w}_k}(\bar{\mathbf{S}}^{(k)})$ denotes a diagonal matrix which can be computed as $(\mathbf{P}_{\mathbf{w}_k}(\bar{\mathbf{S}}^{(k)}))_{ii} = (\bar{\mathbf{S}}^{(k)}_{ii} - w_{ki})_+$, where $(x)_+ = x$ if $x > 0$ and $(x)_+ = 0$ otherwise. w_{ki} is the i-th element of the $\mathbf{w}_k$.

By recalling the definition of WTNN in Definition 5, we have $\frac{1}{\mu_t}\|\boldsymbol{\mathcal{L}}\|_{\mathbf{W},*} = \|\boldsymbol{\mathcal{L}}\|_{\frac{1}{\mu_t}\mathbf{W},*}$. Based on Lemma 1, the solution of the subproblem (17) can be described as

$$\boldsymbol{\mathcal{L}}_{t+1} = \mathbf{Prox}_{\|\cdot\|_{\frac{1}{\mu_t}\mathbf{W},*}}(\boldsymbol{\mathcal{M}} - \boldsymbol{\mathcal{E}}_t - \boldsymbol{\mathcal{Z}}_t/\mu_t). \tag{20}$$

Step2: Update $\boldsymbol{\mathcal{E}}$ by fixing other variables:

$$\boldsymbol{\mathcal{E}}_{t+1} = \arg\min_{\boldsymbol{\mathcal{E}}} \frac{\lambda}{\mu_t}\|\boldsymbol{\mathcal{E}}\|_{\boldsymbol{\mathcal{W}},1}+\frac{1}{2}\|\boldsymbol{\mathcal{E}}-(\boldsymbol{\mathcal{M}}-\boldsymbol{\mathcal{L}}_{t+1}-\boldsymbol{\mathcal{Z}}_t/\mu_t)\|_F^2. \tag{21}$$

To get the closed-form solution of the above problem, we utilize the tensor soft-thresholding operator (**TST**) defined below to update $\boldsymbol{\mathcal{E}}_{t+1}$.

$$\boldsymbol{\mathcal{E}}_{t+1} = \mathbf{TST}(\boldsymbol{\mathcal{M}} - \boldsymbol{\mathcal{L}}_{t+1} - \boldsymbol{\mathcal{Z}}_t/\mu_t, \frac{\lambda}{\mu_t}\boldsymbol{\mathcal{W}}_t), \tag{22}$$

where the ijk-th entry of **TST** is defined by

$$(\mathbf{TST}(\boldsymbol{\mathcal{X}}, \boldsymbol{\mathcal{W}}))_{ijk} = \text{sign}(\boldsymbol{\mathcal{X}}_{ijk})(|\boldsymbol{\mathcal{X}}_{ijk}| - \boldsymbol{\mathcal{W}}_{ijk})_+. \tag{23}$$

Step3: Update the elements of $\mathbf{W}$ and $\boldsymbol{\mathcal{W}}$ by an adaptive way according to Proposition 1

$$(W_{t+1})_{ki} = \xi(\sigma_i(\bar{\mathbf{L}}^{(k)}_{t+1}); c), (\boldsymbol{\mathcal{W}}_{t+1})_{ijk} = \xi(|(\boldsymbol{\mathcal{E}}_{t+1})_{ijk}|; c). \tag{24}$$

Step4: Update the Lagrangian multiplier tensor $\boldsymbol{\mathcal{Z}}$ and the parameter μ by

$$\boldsymbol{\mathcal{Z}}_{t+1} = \boldsymbol{\mathcal{Z}}_t + \mu_t(\boldsymbol{\mathcal{L}}_{t+1} + \boldsymbol{\mathcal{E}}_{t+1} - \boldsymbol{\mathcal{M}}), \tag{25}$$

Algorithm 1 **FGTRPCA algorithm**

Input: Observation tensor data $\boldsymbol{\mathcal{M}} \in \mathbb{R}^{d_1\times d_2\times d_3}$, and the parameter λ.

1: Initialize $\boldsymbol{\mathcal{L}}_0 = \boldsymbol{\mathcal{E}}_0 = \boldsymbol{\mathcal{Z}}_0 = 0$, $\mathbf{W}_0 = \mathbf{1}_{d_3\times d}$, $\boldsymbol{\mathcal{W}}_0 = \mathbf{1}_{d_1\times d_2\times d_3}$, $\mu_0 = 10^{-2}$, $\rho = 1.1$, $\epsilon = 10^{-6}$, and $t = 0$.
2: **while** not converge **do**
3: Update the low-rank tensor $\boldsymbol{\mathcal{L}}$ by Eq. (17).
4: Update the sparse tensor $\boldsymbol{\mathcal{E}}$ by Eq. (21).
5: Update the weights $\mathbf{W}$ and $\boldsymbol{\mathcal{W}}$ by Eq. (24).
6: Update the Lagrangian multiplier $\boldsymbol{\mathcal{Z}}$ by Eq. (25).
7: Update the parameter μ by Eq. (26).
8: Check the convergence condition in Eq. (27).
9: **end while**

Output: $\boldsymbol{\mathcal{L}} = \boldsymbol{\mathcal{L}}_{t+1}, \boldsymbol{\mathcal{E}} = \boldsymbol{\mathcal{E}}_{t+1}$

$$\mu_{t+1} = \rho\mu_t, \tag{26}$$

where $\rho = 1.1$. The convergence conditions are defined as

$$\max\left\{\begin{array}{l}\|\boldsymbol{\mathcal{L}}_{t+1} - \boldsymbol{\mathcal{L}}_t\|_\infty,\\ \|\boldsymbol{\mathcal{E}}_{t+1} - \boldsymbol{\mathcal{E}}_t\|_\infty,\\ \|\boldsymbol{\mathcal{M}} - \boldsymbol{\mathcal{L}}_{t+1} - \boldsymbol{\mathcal{E}}_{t+1}\|_\infty\end{array}\right\} \le \epsilon. \tag{27}$$

The whole optimization procedure is summarized in Algorithm 1.

3.4 Smooth FGTRPCA

Considering a structured tensor that exhibits both low-rankness and smoothness, we devise a novel regularizer that aims to represent both two properties simultaneously on the gradient tensors, instead of employing a combination of two distinct regularizers for encoding the two properties. We first introduce the definition of the gradient tensor and present our proposed tensor-correlated Flexible Generalized Joint Prior (t-FGJP) regularizer.

Definition 7. ***(Gradient tensor)****[Wang* et al.*, 2023a] For a tensor $\boldsymbol{\mathcal{X}} \in \mathbb{R}^{d_1\times d_2\times d_3}$, its gradient tensor along the k-th mode is defined as*

$$\boldsymbol{\mathcal{G}}_k := \nabla_k(\boldsymbol{\mathcal{X}}) = \boldsymbol{\mathcal{X}} \times_k \mathbf{D}_{d_k}, k = 1, 2, 3, \tag{28}$$

where $\mathbf{D}_{d_k}$ is a row circulant matrix of $(-1, 1, 0, ..., 0)$.

Definition 8. ***(t-FGJP)*** *For a tensor $\boldsymbol{\mathcal{X}} \in \mathbb{R}^{d_1\times d_2\times d_3}$, the proposed t-FGJP norm is defined as*

$$\|\boldsymbol{\mathcal{X}}\|_{\text{t-FGJP}} := \frac{1}{\gamma}\sum_{k\in\Gamma}\|\boldsymbol{\mathcal{G}}_k\|_{G,\alpha,*}, \tag{29}$$

where Γ represents a priori set of directions along which $\boldsymbol{\mathcal{X}}$ equips both low-rankness and smoothness priors and $\gamma := \#\{\Gamma\}$ denotes the cardinality of Γ. By incorporating both t-FGJP and FGTL1N into the TRPCA framework, we propose a smooth FGTRPCA (SFGTRPCA) model defined as

$$\min_{\boldsymbol{\mathcal{L}},\boldsymbol{\mathcal{E}}} \|\boldsymbol{\mathcal{L}}\|_{\text{t-FGJP}} + \lambda\|\boldsymbol{\mathcal{E}}\|_{G,\alpha,1} \text{ s.t. } \boldsymbol{\mathcal{M}} = \boldsymbol{\mathcal{L}} + \boldsymbol{\mathcal{E}}. \tag{30}$$

The SFGTRPCA optimization problem is similar to the FGTRPCA problem. Details of the optimization algorithm and the entire procedure are presented in the supplementary material due to space limitations.

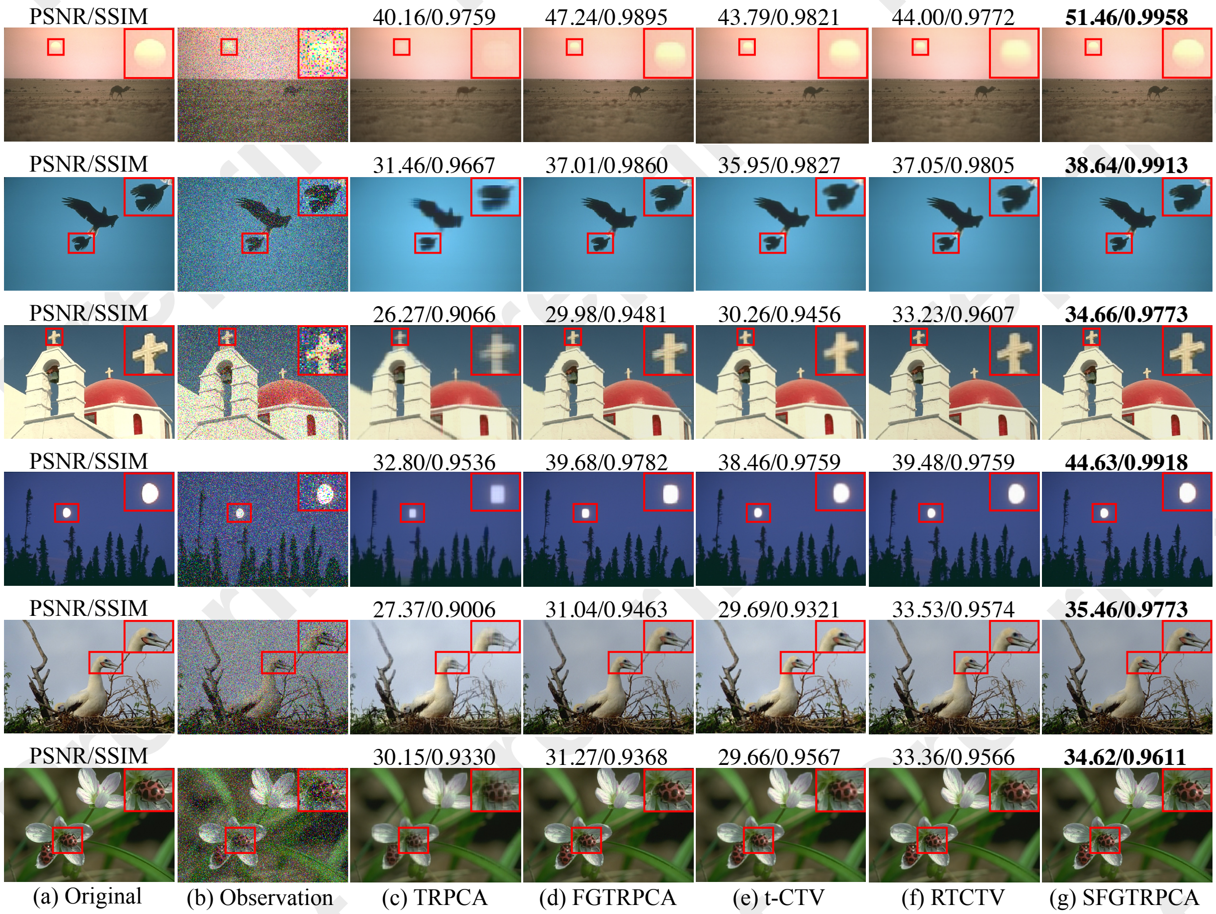

Figure 4: Recovery results on 6 color images from the BSD dataset with 20% noise ratio.

4 Experiments

In this section, we present several real-world experiments to substantiate the effectiveness of our models. Additional results are provided in the supplementary material.

4.1 Settings

Datasets. For comprehensive comparison, we use 4 widely used tensor data types including color images, grayscale videos, hyperspectral images (HSIs), and multispectral images (MSIs). For color images, we choose 3 widely used datasets including Berkeley Segmentation Dataset[1] (BSD) [Martin *et al.*, 2001], Kodak [Kodak, 1993] dataset[2], and ZheJiang University (ZJU) [Hu *et al.*, 2012] dataset[3]. For grayscale videos, we use 14 grayscale video sequences from the YUV dataset[4] and select the first 100 frames for each sequence. For HSIs, we utilize Cuprite[5], DCMall[5], Urban[5], Indian Pines[5], and Pavia University[5] (PaviaU) with their first 50 bands from each HSI dataset for experiments. For MSIs, we randomly select 4 MSIs from the CAVE dataset [Yasuma *et al.*, 2008].

Baselines. Our baselines are divided into two categories based on different priors. (1) Low-rankness: TRPCA [Lu *et al.*, 2020], ETRPCA [Gao *et al.*, 2020], and PTRPCA [Yan and Guo, 2024]; (2) Joint Low-rankness & Smoothness: t-CTV [Wang *et al.*, 2023a] and RTCTV [Huang *et al.*, 2024]. We utilize the parameters recommended by the authors. For the key parameter α in our models, we search from a candidate set and employ $\alpha = 0.5$. More detailed parameter settings are described in the supplementary material.

Evaluation metrics. The peak signal-to-noise ratio (PSNR) and structural similarity (SSIM) are used to evaluate the recovery performance.

Noising Data Construction. For each color channel of the color image, each frame of the grayscale video, and each band of HSI and MSI, we add random salt and pepper noise at varying noise ratios of 10%, 20%, and 30%.

[1]https://www2.eecs.berkeley.edu/Research/Projects/CS/vision/bsds/
[2]http://r0k.us/graphics/kodak/
[3]https://sites.google.com/site/zjuyaohu/
[4]http://trace.eas.asu.edu/yuv/
[5]https://lesun.weebly.com/hyperspectral-data-set.html

	Noise Ratio	10%		20%	
	Methods	**PSNR**	**SSIM**	**PSNR**	**SSIM**
Color images	TRPCA	31.20	0.9464	29.55	0.9115
	ETRPCA	33.26	0.9580	31.23	0.9233
	PTRPCA	33.37	0.9622	31.43	0.9350
	FGTRPCA	37.26	0.9796	33.26	0.9415
	t-CTV	32.84	0.9525	31.71	0.9348
	RTCTV	34.96	0.9689	33.46	0.9529
	SFGTRPCA	**40.96**	**0.9907**	**36.93**	**0.9782**
Grayscale videos	TRPCA	35.19	0.9636	34.16	0.9538
	ETRPCA	38.29	0.9772	36.13	0.9433
	PTRPCA	38.95	0.9807	37.31	0.9669
	FGTRPCA	41.85	0.9858	39.07	0.9743
	t-CTV	37.37	0.9721	36.52	0.9665
	RTCTV	41.11	0.9843	38.62	0.9482
	SFGTRPCA	**44.51**	**0.9911**	**41.91**	**0.9846**
HSIs	TRPCA	44.18	0.9754	42.48	0.9718
	ETRPCA	44.54	0.9747	43.20	0.9720
	PTRPCA	47.38	0.9815	45.48	0.9772
	FGTRPCA	47.30	0.9858	44.90	0.9787
	t-CTV	45.72	0.9779	44.39	0.9759
	RTCTV	48.29	0.9812	46.76	0.9789
	SFGTRPCA	**52.38**	**0.9888**	**50.16**	**0.9856**
MSIs	TRPCA	42.07	0.9898	40.41	0.9867
	ETRPCA	45.95	0.9931	44.00	0.9906
	PTRPCA	46.87	0.9939	44.84	0.9920
	FGTRPCA	49.73	0.9960	46.05	0.9921
	t-CTV	46.62	0.9938	45.21	0.9925
	RTCTV	50.19	0.9952	48.69	0.9941
	SFGTRPCA	**57.37**	**0.9977**	**53.35**	**0.9955**

Table 2: Denoising performance on 4 types of tensor data with varying noise levels, evaluated in terms of average PSNR and SSIM values. The best and second-best results are marked in bold, and the second-best results are underlined.

4.2 Experimental Results

Visual Quality. To clearly illustrate the advantages of our methods on color image recovery, Figure 4 presents 6 sample images from the BSD dataset, along with the recovery results under 20% salt and pepper noise. The PSNR and SSIM values are listed above the recovered images to enhance the credibility of the results. The results show that SFGTRPCA constructs more image details and color information (Especially the contour and color of the moon in the 4-th image). Additionally, we have observed that the proposed FGTRPCA and SFGTRPCA methods significantly outperform the baseline methods under corresponding priors.

Quantitative Quality. Table 2 displays the results of all the competitors on the 4 tensor types with 10% and 20% noise. From the results, we draw the following conclusions:

- Firstly, SFGTRPCA outperforms all comparison methods, achieving an average PSNR improvement of over 4.4 dB compared to the second-best baseline. Specifically, it attains PSNR gains of 17.16% and 14.31% for color images and MSIs with 10% noise, respectively. This is because our model can adaptively learn appropriate weights for the frontal slices of the tensor through a weighting function.
- Secondly, compared to the baselines that only consider the low-rankness prior (TRPCA, ETRPCA, and PTRPCA), our FGTRPCA demonstrates the best performance in most situations, and achieves an average improvement of over 1.7 dB in PSNR compared to the second-best baseline. Notably, our FGTRPCA always leads in SSIM values, which indicates that our FGTRPCA can recover more structural information.
- Thirdly, our methods consistently achieve competitive evaluation scores across diverse tensor data types under varying noise levels, demonstrating their ability to effectively leverage low-rank and sparse structures for robust recovery.

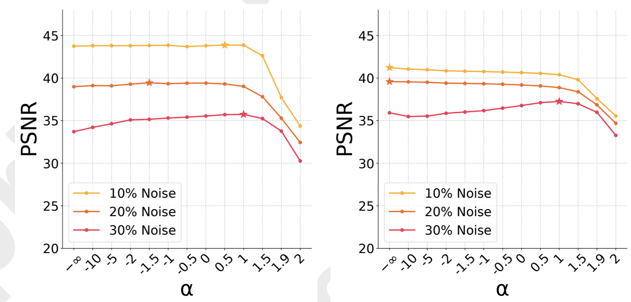

(a) ZJU (color images) (b) Indian Pine (HSIs)

Figure 5: PSNR values of our SFGTRPCA algorithm on different cases. For various values of α, with the point of highest value marked by a pentagram.

Parameter Analysis. It should be noticed that the parameter α plays a crucial role in our models, which can adjust the flexibility and generalizability to adapt to various scenarios. To explore its impact on different cases, we examine some recovery tasks with different values of α under various noise ratios on ZJU (color images) and Indian Pines (HSIs) datasets in Figure 5. As seen, by tuning α, our SFGTRPCA model gains significant improvements in various situations. This improvement highlights the advantage of incorporating α as a hyperparameter instead of a fixed formula and validates the flexibility of our framework.

5 Conclusion

In this article, we propose a flexible generalized low-rank regularizer termed FGTNN, and develop a novel FGTRPCA framework. Many existing TRPCA methods can fall into our special cases, which reveals connections between existing and new TRPCA approaches through a continuous parameter. Additionally, by integrating low-rankness and smoothness priors, we design a novel regularizer based on FGTNN and propose a smooth FGTRPCA (SFGTRPCA) model. Compared to existing works, our models process with flexibility and generalizability, demonstrating superior performance.

Ethical Statement

There are no ethical issues.

Acknowledgments

We are grateful to the anonymous IJCAI reviewers for their constructive comments. This work was supported by the National Natural Science Foundation of China (under Grant Nos. 62276111, 62076041, 61806027, 61702057, and 62202009), the Fundamental Research Funds for the Central Universities of China (under Grant Nos. 2662023XXPY002 and 2662023LXPY005), the HZAU-AGIS Cooperation Fund (under Grant No. SZYJY2023010), and the Industry-University-Research Cooperation Project of Zhuhai, Guangdong, China, under Grant GP/026/2020 and Grant HF-010-2021.

Contribution Statement

Zhiyang Gong and Jie Yu are co-first authors, and Yulong Wang is the corresponding author.

References

[Barron *et al.*, 2023] Jonathan T Barron, Ben Mildenhall, Dor Verbin, Pratul P Srinivasan, and Peter Hedman. Zip-nerf: Anti-aliased grid-based neural radiance fields. In *Proceedings of the IEEE/CVF International Conference on Computer Vision*, pages 19697–19705, 2023.

[Boyd *et al.*, 2011] Stephen Boyd, Neal Parikh, Eric Chu, Borja Peleato, Jonathan Eckstein, et al. Distributed optimization and statistical learning via the alternating direction method of multipliers. *Foundations and Trends® in Machine learning*, 3(1):1–122, 2011.

[Chen *et al.*, 2021] Lin Chen, Xue Jiang, Xingzhao Liu, and Zhixin Zhou. Logarithmic norm regularized low-rank factorization for matrix and tensor completion. *IEEE Transactions on Image Processing*, 30:3434–3449, 2021.

[Gao *et al.*, 2020] Quanxue Gao, Pu Zhang, Wei Xia, Deyan Xie, Xinbo Gao, and Dacheng Tao. Enhanced tensor rpca and its application. *IEEE Transactions on Pattern Analysis and Machine Intelligence*, 43(6):2133–2140, 2020.

[Hou *et al.*, 2024] Jingyao Hou, Xinling Liu, Hailin Wang, and Ke Guo. Tensor recovery from binary measurements fused low-rankness and smoothness. *Signal Processing*, 221:109480, 2024.

[Hu *et al.*, 2012] Yao Hu, Debing Zhang, Jieping Ye, Xuelong Li, and Xiaofei He. Fast and accurate matrix completion via truncated nuclear norm regularization. *IEEE Transactions on Pattern Analysis and Machine Intelligence*, 35(9):2117–2130, 2012.

[Huang *et al.*, 2015] Bo Huang, Cun Mu, Donald Goldfarb, and John Wright. Provable models for robust low-rank tensor completion. *Pacific Journal of Optimization*, 11(2):339–364, 2015.

[Huang *et al.*, 2024] Kai Huang, Weichao Kong, Min Zhou, Wenjin Qin, Feng Zhang, and Jianjun Wang. Enhanced low-rank tensor recovery fusing reweighted tensor correlated total variation regularization for image denoising. *Journal of Scientific Computing*, 99(3):69, 2024.

[Ji and Feng, 2023] Jintian Ji and Songhe Feng. Anchor structure regularization induced multi-view subspace clustering via enhanced tensor rank minimization. In *Proceedings of the IEEE/CVF International Conference on Computer Vision*, pages 19343–19352, 2023.

[Jiang *et al.*, 2020] Tai-Xiang Jiang, Ting-Zhu Huang, Xi-Le Zhao, and Liang-Jian Deng. Multi-dimensional imaging data recovery via minimizing the partial sum of tubal nuclear norm. *Journal of Computational and Applied Mathematics*, 372:112680, 2020.

[Kilmer and Martin, 2011] M. Kilmer and C. Martin. Factorization strategies for third-order tensors. *Linear Algebra Appl.*, 435(3):641–658, 2011.

[Kilmer *et al.*, 2013] Misha E Kilmer, Karen Braman, Ning Hao, and Randy C Hoover. Third-order tensors as operators on matrices: A theoretical and computational framework with applications in imaging. *SIAM Journal on Matrix Analysis and Applications*, 34(1):148–172, 2013.

[Kilmer *et al.*, 2021] Misha E Kilmer, Lior Horesh, Haim Avron, and Elizabeth Newman. Tensor-tensor algebra for optimal representation and compression of multiway data. *Proceedings of the National Academy of Sciences*, 118(28):e2015851118, 2021.

[Ko *et al.*, 2020] Ching-Yun Ko, Kim Batselier, Lucas Daniel, Wenjian Yu, and Ngai Wong. Fast and accurate tensor completion with total variation regularized tensor trains. *IEEE Transactions on Image Processing*, 29:6918–6931, 2020.

[Kodak, 1993] Eastman Kodak. Kodak lossless true color image suite (photocd pcd0992). *URL http://r0k. us/graphics/kodak*, 6:2, 1993.

[Liu *et al.*, 2024a] Youfa Liu, Bo Du, Yongyong Chen, Lefei Zhang, Mingming Gong, and Dacheng Tao. Convex–concave tensor robust principal component analysis. *International Journal of Computer Vision*, 132(5):1721–1747, 2024.

[Liu *et al.*, 2024b] Youheng Liu, Yulong Wang, Longlong Chen, Libin Wang, and Yutao Hu. Tihn: Tensor improved huber norm for low-rank tensor recovery. *International Journal of Wavelets, Multiresolution and Information Processing*, 22(05):2450023, 2024.

[Liu *et al.*, 2024c] Zhiyu Liu, Zhi Han, Yandong Tang, Xi-Le Zhao, and Yao Wang. Low-tubal-rank tensor recovery via factorized gradient descent. *arXiv preprint arXiv:2401.11940*, 2024.

[Lu *et al.*, 2020] C. Lu, J. Feng, Y. Chen, W. Liu, Z. Lin, and S. Yan. Tensor robust principal component analysis with a new tensor nuclear norm. *IEEE Transactions on Pattern Analysis and Machine Intelligence*, 42(4):925–938, Apr. 2020.

[Martin *et al.*, 2001] David Martin, Charless Fowlkes, Doron Tal, and Jitendra Malik. A database of human segmented natural images and its application to evaluating segmentation algorithms and measuring ecological statistics. In *Proceedings eighth IEEE international conference on computer vision. ICCV 2001*, volume 2, pages 416–423. IEEE, 2001.

[Peng *et al.*, 2020] Jiangjun Peng, Qi Xie, Qian Zhao, Yao Wang, Leung Yee, and Deyu Meng. Enhanced 3dtv regularization and its applications on hsi denoising and compressed sensing. *IEEE Transactions on Image Processing*, 29:7889–7903, 2020.

[Peng *et al.*, 2022a] Jiangjun Peng, Hailin Wang, Xiangyong Cao, Xinling Liu, Xiangyu Rui, and Deyu Meng. Fast noise removal in hyperspectral images via representative coefficient total variation. *IEEE Transactions on Geoscience and Remote Sensing*, 60:1–17, 2022.

[Peng *et al.*, 2022b] Jiangjun Peng, Yao Wang, Hongying Zhang, Jianjun Wang, and Deyu Meng. Exact decomposition of joint low rankness and local smoothness plus sparse matrices. *IEEE Transactions on Pattern Analysis and Machine Intelligence*, 45(5):5766–5781, 2022.

[Phothilimthana *et al.*, 2024] Mangpo Phothilimthana, Sami Abu-El-Haija, Kaidi Cao, Bahare Fatemi, Michael Burrows, Charith Mendis, and Bryan Perozzi. Tpugraphs: A performance prediction dataset on large tensor computational graphs. *Advances in Neural Information Processing Systems*, 36, 2024.

[Qin *et al.*, 2024] Wenjin Qin, Hailin Wang, Feng Zhang, Weijun Ma, Jianjun Wang, and Tingwen Huang. Nonconvex robust high-order tensor completion using randomized low-rank approximation. *IEEE Transactions on Image Processing*, 33:2835–2850, 2024.

[Qiu *et al.*, 2021] Duo Qiu, Minru Bai, Michael K Ng, and Xiongjun Zhang. Robust low-rank tensor completion via transformed tensor nuclear norm with total variation regularization. *Neurocomputing*, 435:197–215, 2021.

[Wang *et al.*, 2023a] Hailin Wang, Jiangjun Peng, Wenjin Qin, Jianjun Wang, and Deyu Meng. Guaranteed tensor recovery fused low-rankness and smoothness. *IEEE Transactions on Pattern Analysis and Machine Intelligence*, 45(9):10990–11007, 2023.

[Wang *et al.*, 2023b] Yulong Wang, Kit Ian Kou, Hong Chen, Yuan Yan Tang, and Luoqing Li. Double auto-weighted tensor robust principal component analysis. *IEEE Transactions on Image Processing*, 32:5114–5125, 2023.

[Wen *et al.*, 2024] Tao Wen, Elynn Chen, and Yuzhou Chen. Tensor-view topological graph neural network. In *International Conference on Artificial Intelligence and Statistics*, pages 4330–4338. PMLR, 2024.

[Yan and Guo, 2024] Tinghe Yan and Qiang Guo. Tensor robust principal component analysis via dual lp quasi-norm sparse constraints. *Digital Signal Processing*, 150:104520, 2024.

[Yasuma *et al.*, 2008] Fumihito Yasuma, Tomoo Mitsunaga, Daisuke Iso, and Shree K Nayar. Generalized assorted pixel camera: Post-capture control of. *Tech. rep., Department of Computer Science, Columbia University CUCS-061-08*, 2008.

[Zhang *et al.*, 2023a] Chao Zhang, Huaxiong Li, Wei Lv, Zizheng Huang, Yang Gao, and Chunlin Chen. Enhanced tensor low-rank and sparse representation recovery for incomplete multi-view clustering. In *Proceedings of the AAAI conference on artificial intelligence*, volume 37, pages 11174–11182, 2023.

[Zhang *et al.*, 2023b] Feng Zhang, Hailin Wang, Wenjin Qin, Xile Zhao, and Jianjun Wang. Generalized nonconvex regularization for tensor rpca and its applications in visual inpainting. *Applied Intelligence*, 53(20):23124–23146, 2023.

[Zhao *et al.*, 2024] Linqing Zhao, Xiuwei Xu, Ziwei Wang, Yunpeng Zhang, Borui Zhang, Wenzhao Zheng, Dalong Du, Jie Zhou, and Jiwen Lu. Lowrankocc: Tensor decomposition and low-rank recovery for vision-based 3d semantic occupancy prediction. In *Proceedings of the IEEE/CVF Conference on Computer Vision and Pattern Recognition*, pages 9806–9815, 2024.